Loss of a *FYN*-regulated differentiation and growth arrest pathway in advanced stage neuroblastoma

Bernd Berwanger,[1] Oliver Hartmann,[2] Eckhard Bergmann,[3] Sandra Bernard,[1] Dirk Nielsen,[1] Michael Krause,[1] Ali Kartal,[3] Daniel Flynn,[4] Ruprecht Wiedemeyer,[5] Manfred Schwab,[5] Helmut Schäfer,[2] Holger Christiansen,[3] and Martin Eilers[1,6]

[1]Institute for Molecular Biology and Tumor Research (IMT), Emil-Mannkopff-Strasse 2, 35037 Marburg, Germany
[2]Institute of Medical Biometry and Epidemiology, Bunsenstrasse 3, 35037 Marburg, Germany
[3]Children's Hospital, Deutschhausstrasse 12, 35037 Marburg, Germany
[4]The Mary Babb Randolph Cancer Center and the Department of Microbiology, Immunology and Cell Biology, West Virginia University, Morgantown, West Virginia 26506
[5]Department of Cytogenetics (H0400), German Cancer Research Center, Im Neuenheimer Feld 280, 69120, Heidelberg, Germany
[6]Correspondence: eilers@imt.uni-marburg.de

Summary

Tumor stage, age of patient, and amplification of *MYCN* predict disease outcome in neuroblastoma. To gain insight into the underlying molecular pathways, we have obtained expression profiles from 94 primary neuroblastoma specimens. Advanced tumor stages show a characteristic expression profile that includes downregulation of multiple genes involved in signal transduction through Fyn and the actin cytoskeleton. High expression of Fyn and high Fyn kinase activity are restricted to low-stage tumors. In culture, expression of active Fyn kinase induces differentiation and growth arrest of neuroblastoma cells. Expression of Fyn predicts long-term survival independently of *MYCN* amplification. Amplification of *MYCN* correlates with deregulation of a distinct set of genes, many of which are target genes of Myc. Our data demonstrate a causal role for Fyn kinase in the genesis of neuroblastoma.

Introduction

Human neuroblastoma is a childhood tumor of the peripheral sympathetic nervous system with a cumulative incidence of 16.9 cases per 100,000 children. The course of the disease varies strongly in individual patients, ranging from spontaneous regression to progressive disease and metastasis.

One genetic factor that predicts poor prognosis is the amplification of *MYCN*; enhanced expression of *MYCN*, as a consequence of amplification, contributes to the progression of neuroblastoma (Schwab et al., 1983; Brodeur et al., 1984). The protein encoded by *MYCN* (N-Myc) is a transcription factor, which can both positively and negatively control gene expression (Eisenman, 2001). Models largely derived from tissue culture experiments view Myc proteins as regulators of both cell growth and proliferation (e.g., Elend and Eilers, 1999); whether such models apply to human tumors remains unclear.

Little is known about molecular factors that influence the development of tumors lacking amplified *MYCN*. One such factor is the expression of *HTERT*, encoding the catalytic subunit of telomerase (Hiyama et al., 1995). Elevated expression of *HTERT* predicts poor survival, strongly suggesting that telomere attrition limits tumor growth in vivo. A second factor is the differential expression of members of the trk family of neurotrophin receptors: whereas expression of *TRKA* correlates with good prognosis, expression of *TRKB* indicates poor long-term survival (Nakagawara et al., 1992, 1993). Signaling through TrkA negatively regulates tumorigenicity of human neuroblastoma cells in a xenograft model, arguing that the differential expression through trk receptors is causally involved in neuroblastoma development (Eggert et al., 2002).

Current clinical protocols use tumor stage and age of patient in addition to amplified *MYCN* for prognosis and for decision on therapeutic regimens (Berthold et al., 1997). Like increased age, advanced tumor stage is a strong predictor of poor survival. But whether different tumor stages show consistent genetic differences, and whether such differences reflect alterations in signaling pathways that control neuroblastoma proliferation and differentiation, is not clear.

We have now used cDNA microarray analysis of multiple primary tumor biopsies to deduce expression profiles that characterize both *MYCN* amplified tumors and nonamplified tumors

SIGNIFICANCE

Human neuroblastoma is a childhood tumor with a wide range of clinical outcomes, ranging from spontaneous regression to tumor progression and metastasis. We have used microarray analysis of primary tumor biopsies to obtain expression profiles and dissect signaling pathways that control neuroblastoma development. Our data identify signal transduction through Fyn kinase as a novel pathway that controls neuroblastoma cell differentiation and proliferation. Potentially, the results point to novel therapeutic strategies that can be used in treating the disease.

Table 1. Comparison of the clinical parameters of the 94 patients to the parameters of the 1378 tumors in the collection

Tumor included in the analysis (n = 94)						
	1	2	3	4	4S	All
MYCN nonamplified	19	8	17	21	12	77
MYCN amplified	1	1	4	8	3	17
% MYCN amplified	5	11.1	19	27.6	20	18.1
Age ≤ 12 months	18	1	11	5	15	50
Age > 12 months	2	8	10	24	0	44
Mean (months)	4.3	23.4	28.7	42.6	4	23.3
% of all tumors	21.3	9.6	22.3	30.9	16	100
Tumor collection (n = 1378)						
	1	2	3	4	4S	All
MYCN nonamplified	307	171	233	331	141	1183
MYCN amplified	10	7	49	122	16	204
% MYCN amplified	3.2	3.9	17.4	26.9	10.2	14.7
Age ≤ 12 months	162	70	82	66	157	537
Age > 12 months	155	108	200	387	0	850
Mean (months)	10.8	14.2	17.9	34.3	2.6	34.5
% of all tumors	22.9	12.8	20.3	32.7	11.3	100

of different stages. We find that both *MYCN* amplified tumors and advanced tumor stages are characterized by distinct expression profiles. Specifically, our data identify signaling through the Fyn nonreceptor kinase as a pathway that is downregulated in advanced tumor stages in vivo and controls cellular differentiation in vitro.

Results

In order to gain insights into the molecular pathways governing neuroblastoma development, we obtained expression profiles from 94 individual tumor biopsies using a 4608 cDNA human unigene chip. Each chip was hybridized to cDNA derived from a human neuroblastoma cell line (SHEP) as reference. The tumors were selected to reflect distribution of tumor stages and *MYCN* amplification in the total tumor bank of 1378 tumors (Table 1). To permit interspot and interarray comparisons, each signal was background corrected, and $\log_2$ transformed red/green intensity ratios were calculated and standardized. Two-sample t statistics and adjusted p values were used to identify differentially expressed genes (Callow et al., 2000). The adjusted p values correct for testing 4608 genes at the same time and estimate the overall probability of detecting one false gene (see Experimental Procedures).

Initial analysis revealed that, of the non-*MYCN* amplified tumors, stages 1 and 4, but not stages 2, 3, and 4S, showed distinct expression profiles when compared with the remainder of the tumors (data not shown). We found 24 significant genes differentially expressed between stage 1 (n = 19) and stage 4 (n = 21) tumors (adjusted p value < 0.05). 12 additional genes had an adjusted p value between p = 0.05 and 0.2 (Figure 1). Unsupervised cluster analysis shows that all but three tumors were correctly assigned to the respective stage. Surprisingly, a significant percentage of genes that were differentially expressed encoded genes involved in signaling through the nonreceptor tyrosine kinase Fyn and the actin cytoskeleton. These genes were coordinately downregulated in advanced stage neuroblastoma, both in *MYCN* amplified and nonamplified tumors (Figures 2A and 2B). The group includes *FYN* itself; actin-filament binding protein (*AFAP*), a protein that binds to and activates Src and Fyn kinase (Baisden et al., 2001); α-catenin (*CTNNA1*), whose binding to β- and γ-catenin is regulated through Fyn-dependent phosphorylation (Calautti et al., 1998); neural cell adhesion protein (*NRCAM*), which signals through nonreceptor tyrosine kinases (Ignelzi et al., 1994); and the actin binding proteins tropomodulin (Gregorio et al., 1995) and myristoylated alanine-rich C kinase substrate (*MARCKS*) (Brouns et al., 2000; Yarmola et al., 2001).

In order to validate these data, we randomly picked 16 stage 1 and stage 4 out of the 94 tumors and measured the expression of *FYN* and *AFAP* by quantitative PCR; the results confirmed the differences in mRNA expression detected in the microarray analysis (Supplemental Figure S1A at http://www.cancercell.org/cgi/content/full/2/5/377/DC1). To extend these results, we used Western blotting to measure levels of Fyn protein in a group of 70 tumors; only five of these tumors were included in the array analysis. The levels of Fyn protein varied widely between different tumors (Figure 3A). As expected from the microarray analysis, expression of Fyn strictly correlated with tumor stage, being detectable in most stage 1 tumors and absent from most stage 4 tumors (Figure 3B). Consistent with the microarray data, low expression of Fyn was also observed in *MYCN* amplified tumors (most of which are from stages 3 and 4), arguing that downregulation of Fyn in advanced tumor stages occurs independently of *MYCN* amplification (see below). In parallel, we picked 22 stage 1 and stage 4 tumors out of the group of 70 tumors and determined Fyn kinase activity in extracts using immune-complex kinase assays, measuring both autophosphorylation of Fyn and phosphorylation of the exogenous substrate, enolase (Figures 3C and 3D). In agreement with the results obtained in Western blots, high Fyn kinase activity was consistently observed in biopsies from stage 1 tumors. In contrast, Fyn kinase activity was on average much lower in extracts from stage 4 tumors. The p values for this distribution are below p = 0.001, both for phosphorylation of enolase and for autophosphorylation of Fyn. Fyn kinase activity closely paralleled expression levels when both kinase activity and protein levels were measured from the same tumor (compare Figures 3A and 3C), suggesting that regulation of *FYN* expression is the major factor determining Fyn activity in these extracts. We

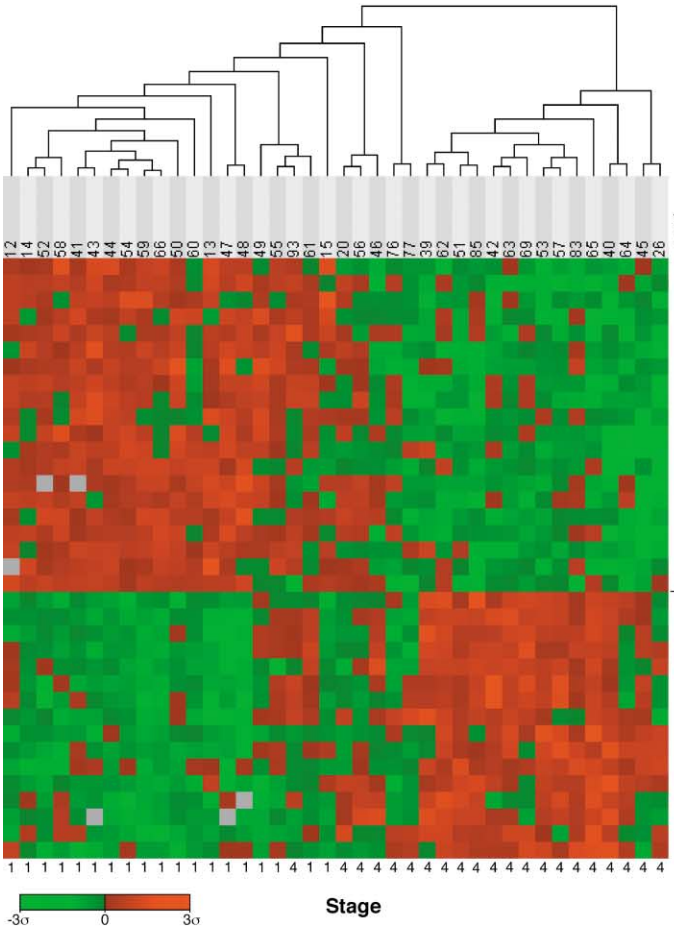

fold regulation	p-value	Gene Name	Accession	C	M	P	S
2,13	<0,01	diacylglycerol kinase, delta (130kD)	AA280692				
3,84	<0,01	EST	H11658				
1,63	0,01	solute carrier family 23, member 1	AA461071				
3,64	0,03	pleiomorphic adenoma gene-like 1	AA463204				
1,53	0,20	hypothetical protein PP3501	N73762				
2,30	<0,01	SOCS box-containing WD protein, SWIP-1	N57723				
1,58	0,06	alpha-catenin	T29500				
1,87	<0,01	FYN oncogene	N66144				
1,80	0,04	v-ral simian leukemia viral oncogene homolog B	W15297				
2,32	0,17	tropomodulin	AA235388				
1,87	<0,01	EST	H48099				
1,74	<0,01	actin filament associated protein	R69356				
1,50	0,06	cyclin T2	R63702				
2,26	0,03	EST	H91164				
3,02	0,17	neuronal cell adhesion molecule	R45583				
1,98	0,05	cDNA FLJ12900 fis	H68664				
1,55	0,05	clone FBD3	R93715				
1,58	<0,01	GL004	W76342				
2,02	0,13	EST	R66946				
1,80	<0,01	KIAA0164	H21107				
2,27	<0,01	ornithine decarboxylase 1	AA461467				
2,62	0,03	EST	N70010				
2,09	0,12	polymyositis/scleroderma autoantigen 1 (75kD)	AA458994				
2,40	0,09	ubiquitin carrier protein E2-C	AA430504				
2,09	0,20	L2DTL protein	R06900				
1,73	0,03	damage-specific DNA binding protein 2	AA410404				
1,70	0,12	diphtheria toxin receptor	R45640				
2,43	<0,01	Mad2	AA481076				
1,67	<0,01	protein phosphatase 1, alpha isoform	AA443982				
2,18	0,05	H1 histone family, member 2	T66815				
1,48	0,04	HSPC023 protein	W92964				
3,08	0,01	EST	T95274				
2,04	0,03	EST	R22212				
2,51	0,10	EST	R70541				
1,39	0,06	DKFZP434C128 protein	AA062813				
1,46	0,11	chromosome 14 ORF 2	T90621				

Figure 1. Identification of a tumor-stage-specific pattern of gene expression

Hierarchical cluster analysis of 21 stage 4 versus 19 stage 1 *MYCN* nonamplified tumors using 36 genes (adjusted p value < 0.2) differentially expressed between stage 4 and stage 1 tumors. Both genes and individual tumors are clustered in this diagram. Green designates downregulation of a gene in a given tumor; red designates upregulation relative to the mean. The standard deviation (σ) from the mean is indicated. Gray spots indicate missing data. The table at the right provides the fold regulation, adjusted p value, and a functional annotation for each gene. The numbers at the top identify the individual tumors. C, genes involved in cell cycle and checkpoints; M, genes involved in metabolism; P, protein synthesis; S, signal transduction.

concluded that expression of Fyn closely parallels tumor stage in human neuroblastoma.

Importantly, the biopsies subjected to Western blotting were derived from patients having a median observation time of 94.1 months, allowing us to evaluate the prognostic value of Fyn expression. In a Kaplan-Meier analysis, expression of Fyn predicted survival with a p value of $p = 2 \times 10^{-4}$ for the total group of 70 tumors and of $p = 0.00694$ for the subset of nonamplified tumors ($n = 58$) (Figure 4A). Multivariate analysis with two parameters showed that expression of *FYN* predicted survival independently of *MYCN* amplification and was a better indicator of prognosis than patient age (Figure 4B). As expected from the analysis, expression of Fyn was strongly correlated to tumor stage and did not predict survival independently of stage.

To test whether *FYN* has a causal role in differentiation and regulation of cell proliferation of neuroblastoma cells, we used transient transfection to express Fyn in SH-SY5Y cells, a human neuroblastoma cell line derived from a stage 4 tumor (Pahlman et al., 1981). Expression of wild-type Fyn (Fynwt) induced the extension of multiple neurites and overt morphological characteristics of differentiation. In contrast, expression of a kinase-negative allele (FynK299M) did not induce morphological differentiation (Figure 5A; a quantitation of the results is shown in Figure 5B). Coexpression of Fyn together with a membrane-localized form of green fluorescent protein (EGFPF, carrying the ras farnesylation signal; Jiang and Hunter, 1998) confirmed that the apparent differences in cell morphology were not due to differential localization of Fynwt and FynK299M (Figure 5A).

In order to demonstrate that the observed changes indeed reflect a neuronal differentiation process, we stained transfected cells with an antibody directed against GAP43, a protein that is abundant in developing neurons and that has been causally implicated in the differentiation of neuroblastoma cells (e.g., Morton and Buss, 1992). Expression of Fynwt strongly upregulated expression of GAP43; in contrast, all cells expressing FynK299M remained negative for GAP43 expression (Figure 5E). Labeling of cells with BrdU or staining with antibodies directed against cyclin A as a marker of cell proliferation revealed that cells expressing active Fyn had exited from the cell cycle (Figure 5C). FACSscan analysis showed that cells expressing Fyn accu-

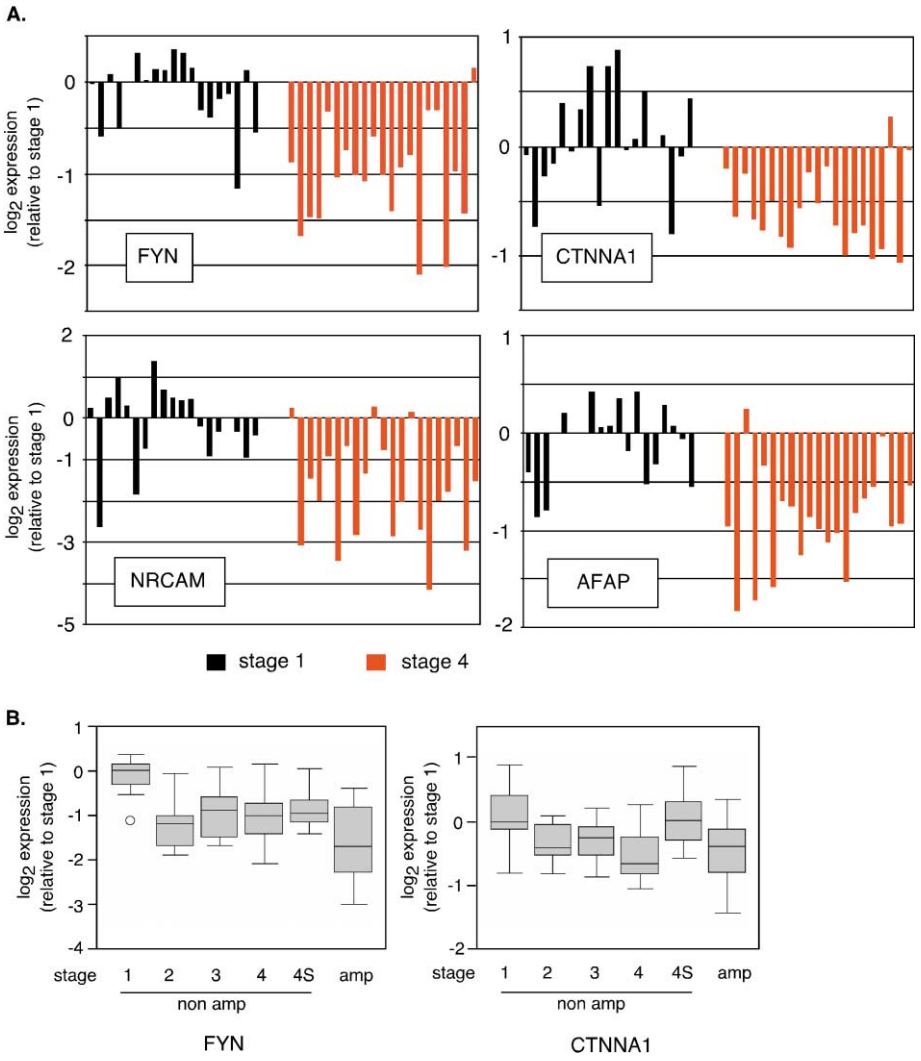

Figure 2. Stage-specific expression of *FYN*, *CTNNA1*, *NRCAM*, and *AFAP*

A: Expression profiles of the indicated genes in stage 1 and stage 4 non-*MYCN*-amplified tumors. All plots show $\log_2$ expression values relative to stage 1.

B: Box plots documenting the distribution of *FYN* and α-catenin (*CTNNA1*) expression in nonamplified tumors of different stages and in tumors carrying amplified *MYCN*. The symbols used in the box plots are explained in the Experimental Procedures.

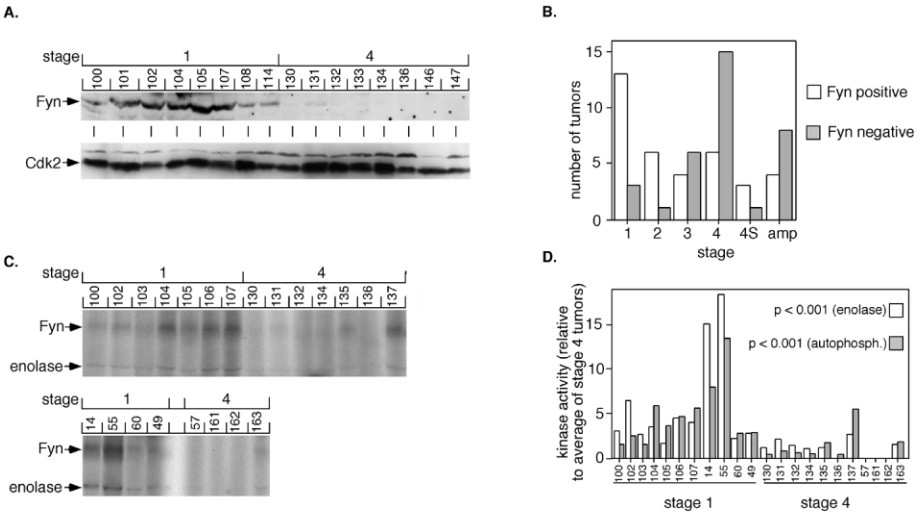

Figure 3. Regulation of Fyn kinase expression and activity in neuroblastoma stages

A: The upper panel shows a Western blot analysis of 16 (out of 70 tested) tumors documenting differential expression of Fyn protein in stage 1 versus stage 4 tumors. Expression of Cdk2 was used as a control (lower panel). The numbers identify the individual tumors. The tumors were selected to document expression differences of Fyn protein between tumors scored as negative and positive (all stage 1 tumors and tumor 131).

B: Expression of Fyn protein is correlated with tumor stage. The panel shows the number of tumors scored as negative or positive for Fyn expression in a group of 70 tumors in relation to tumor stage.

C: Immune-complex kinase assays documenting Fyn kinase activity measured either as Fyn autophosphorylation or as phosphorylation of enolase (see arrows) in 22 stage 1 and stage 4 tumors.

D: Quantitation of the results shown in **C**. Shown is the kinase activity in each tumor relative to the average activity in stage 4 tumors.

A.

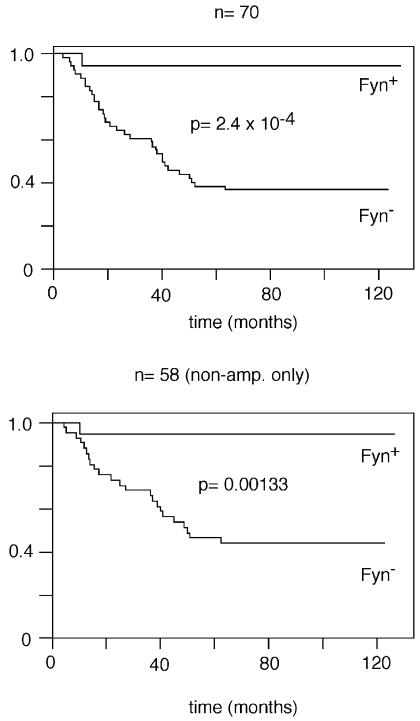

B.

Independent variable		p-value	
1st	2nd	1st var	2nd var
MYCN		**< 0.001**	
Fyn		**0.002**	
age		**0.006**	
stage		**< 0.001**	
Fyn	**MYCN**	**0.007**	**< 0.001**
Fyn	age	**0.012**	0.066
Fyn	**stage**	0.069	**< 0.001**

Figure 4. Expression of Fyn is prognostic for long-term survival of neuroblastoma patients

A: Kaplan-Meier diagrams documenting increased survival probability of patients with tumors that contain detectable amounts of Fyn (Fyn^+) versus patients with tumors lacking detectable Fyn (Fyn^-). The upper diagram shows survival probability in the total group of 70 tumors that were analyzed; the lower diagram shows survival probability in the 58 tumors that lack amplified *MYCN*.

B: Multivariate analysis using the parameters age, stage, Fyn expression, and amplification of *MYCN*. Statistically significant parameters are shown in bold.

mulated in the G1 phase of the cell cycle (Figure 5D). We concluded that Fyn induces G1 arrest and neuronal differentiation of neuroblastoma cells. Consistent with a role of AFAP in activation of Fyn, expression of a constitutively active allele of AFAP induced morphological changes highly reminiscent of active Fyn, while a dominant negative allele of AFAP did not affect differentiation (not shown).

We repeated the experiments in IMR-32 cells, a human neuroblastoma cell line that carries amplified *MYCN* (Clementi et al., 1986). Similar to results obtained in SH-SY5Y cells, expression of active Fyn kinase induced neurite extension and cell cycle exit (Figure 5F). We concluded that the induction of differentiation by Fyn occurs even in the presence of amplified *MYCN*.

Expression of *FYN* did not discriminate between tumors that do or do not have amplified *MYCN* ($p = 0.558$ in the whole group of 94 tumors; $p = 1.0$ when adjusted for stage; see also Figure 2B). Also, the multivariate analysis showed that amplification of *MYCN* and expression of *FYN* are independently prognostic for survival (Figure 4). Together, both findings strongly suggest that amplification of *MYCN* does not promote tumor progression through regulation of *FYN* expression. We therefore wondered whether there are genes that are specifically deregulated in *MYCN* amplified tumors. We found 123 differentially expressed genes when comparing *MYCN* amplified ($n = 17$) and nonamplified ($n = 77$) tumors (adjusted p value < 0.05). Using these genes in an unsupervised, hierarchical cluster analysis showed that all but two tumors were correctly assigned to one of the two classes (see Supplemental Figure S2 at http://www.cancercell.org/cgi/content/full/2/5/377/DC1). With two exceptions (*SWIP1* and *MAD2*), this set of genes showed no overlap with the group of genes that discriminates stage 1 from stage 4 tumors. In order to validate these observations, we measured the expression of *AUROR2*, *MYCN*, and *HSP75* in 16 randomly picked amplified and nonamplified tumors using quantitative PCR (see Supplemental Figure S1B); the results confirmed the expression differences observed in the microarray analysis.

Functional annotation showed that most genes that were upregulated in *MYCN* amplified tumors encoded proteins that function in protein synthesis, metabolism, and cell cycle regulation (see Supplemental Figure S2); this is consistent with microarray data using inducible systems in tissue culture (Coller et al., 2000; Guo et al., 2000; Menssen and Hermeking, 2002; O'Hagan et al., 2000; Schuhmacher et al., 2001). The findings strongly support the notion that Myc proteins regulate both cell growth and cell proliferation and argue that models developed in tissue culture extend to the genesis of neuroblastoma (Beier et al., 2000; Eilers et al., 1991; Johnston et al., 1999; Schuhmacher et al., 1999). A large group of genes that were mostly downregulated in *MYCN* amplified tumors encoded proteins involved in multiple signal transduction pathways, supporting the notion that Myc proteins provide a negative feedback signal to signaling pathways (Supplemental Figure S2) (Oster et al., 2000). Surprisingly, the cell cycle genes that were upregulated in *MYCN* amplified tumors encode proteins known to function in checkpoint responses or in the G2 and M phases of the cycle, pointing to novel functions of Myc in checkpoint control and late in the cell cycle (Figure 6A) (see also Menssen and Hermeking, 2002).

To formally show that deregulation of these genes does not simply reflect the advanced tumor stage of most *MYCN* amplified tumors, we compared their expression between stage 4 *MYCN* amplified and nonamplified tumors (Figure 6B). The

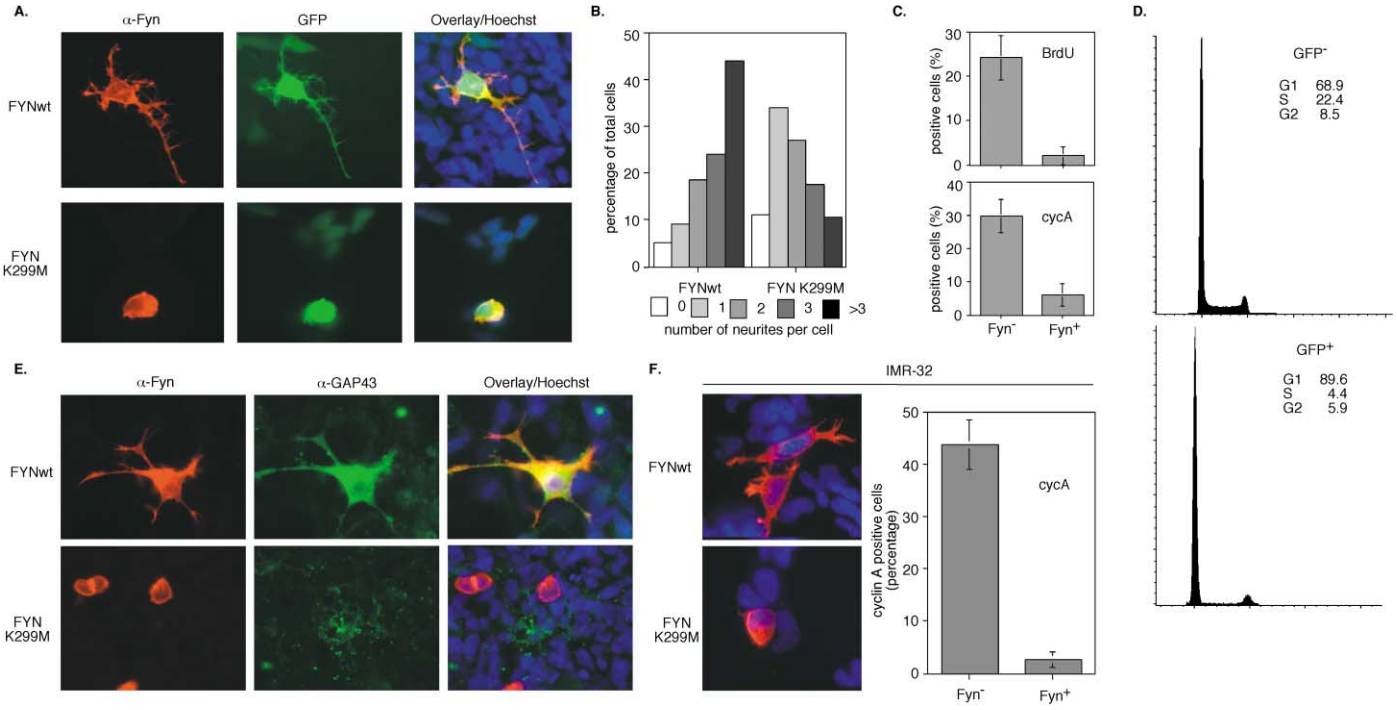

Figure 5. Regulation of neuroblastoma cell differentiation and proliferation by Fyn

A: Immunofluorescence pictures of SH-SY5Y cells showing the morphology of representative cells transfected with expression plasmids encoding Fynwt (upper three panels) or FynK299M (lower three panels) together with a plasmid encoding a GFP that is targeted to the plasma membran (EGFPF). Left panels show staining with an antibody directed against Fyn, middle panels show GFP fluorescence, and right panels show the overlay together with Hoechst staining to visualize nuclei.

B: Quantitation of the results obtained. Shown is the percentage of cells with the indicated numbers of neurites after transfection with the indicated expression plasmids (100 Fyn-positive cells were counted for each experiment).

C: Percentage of cells incorporating BrdU (upper panel) or staining positive for cyclin A (lower panel) of SH-SY5Y cells transfected with an expression vector encoding Fynwt. Cells were stained both for Fyn and for cyclin A or BrdU and Fyn-positive and -negative cells were counted separately.

D: FACSscan analysis documenting accumulation in the G1 phase of the cell cycle of SH-SY5Y cells expressing Fyn. Cells were transfected with a plasmid encoding a Fyn-GFP chimerical protein and subjected to cell cycle analysis (using propidium iodide staining) after gating for GFP-positive and -negative cells.

E: Immunofluorescence pictures of SH-SY5Y cells showing expression of GAP43 in cells expressing Fynwt (upper panels) but not in cells expressing FynK299M (lower panels). The right panels show cells stained with an antibody directed against Fyn, the middle panels show staining with an α-GAP43 antibody, and the right panels show the overlay together with Hoechst staining to visualize nuclei.

F: The left panels show immunofluorescence pictures documenting the morphology of IMR-32 cells upon expression of Fynwt or FynK299M. The right panel documents the percentage of IMR-32 cells expressing cyclin A.

expression of all genes that we analyzed was regulated by *MYCN* amplification independent of tumor stage. Conversely, deregulation of expression might be a consequence of *MYCN* amplification. Indeed, expression of a panel of genes identified as target genes of (c-)Myc in tissue culture experiments was significantly different between both classes of tumors (Figure 6C).

To extend these observations, we asked whether additional genes contained on the list are target genes that are regulated by N-Myc. In order to address this question, we analyzed the expression of eight randomly chosen genes in a cell line that carries a tetracycline regulatable allele of N-Myc (Lutz et al., 1996). Of those, six genes were induced in response to induction of *MYCN* expression (Figure 6D); no regulation was observed for two genes (*EFNB3* and *SWIP1*), suggesting that their deregulation in *MYCN* amplified tumors may reflect events in tumorigenesis that cannot be mimicked in tissue culture. In addition, we did not observe any regulation of *FYN* expression by *MYCN* in this cell line (Figure 6D).

To determine whether some of these genes are indeed direct targets of N-Myc, we searched for potential binding sites for N-Myc (E boxes) in the promoter region and introns of the six regulated genes. Potential N-Myc binding sites were found in four of them (Figure 6E and data not shown). We then performed chromatin-immunoprecipitation experiments, using the prothymosin-α gene (*PTMA*, see Figure 6B) as positive control. In vivo binding of N-Myc was detected to E boxes in the *MAD2*, *HSP75*, and *FACL2* genes, strongly suggesting that they are directly regulated by N-Myc in vivo (Figure 6E). No binding was detected to the E boxes in the *AURORA2* gene. Taken together, our data suggest that a significant fraction of the genes that discriminate *MYCN* amplified from nonamplified tumors are regulated as a consequence of *MYCN* amplification, since they are direct or indirect targets for transcriptional regulation by N-Myc.

Discussion

Previous work has identified amplification of *MYCN* as a genetic event that strongly affects neuroblastoma development. While

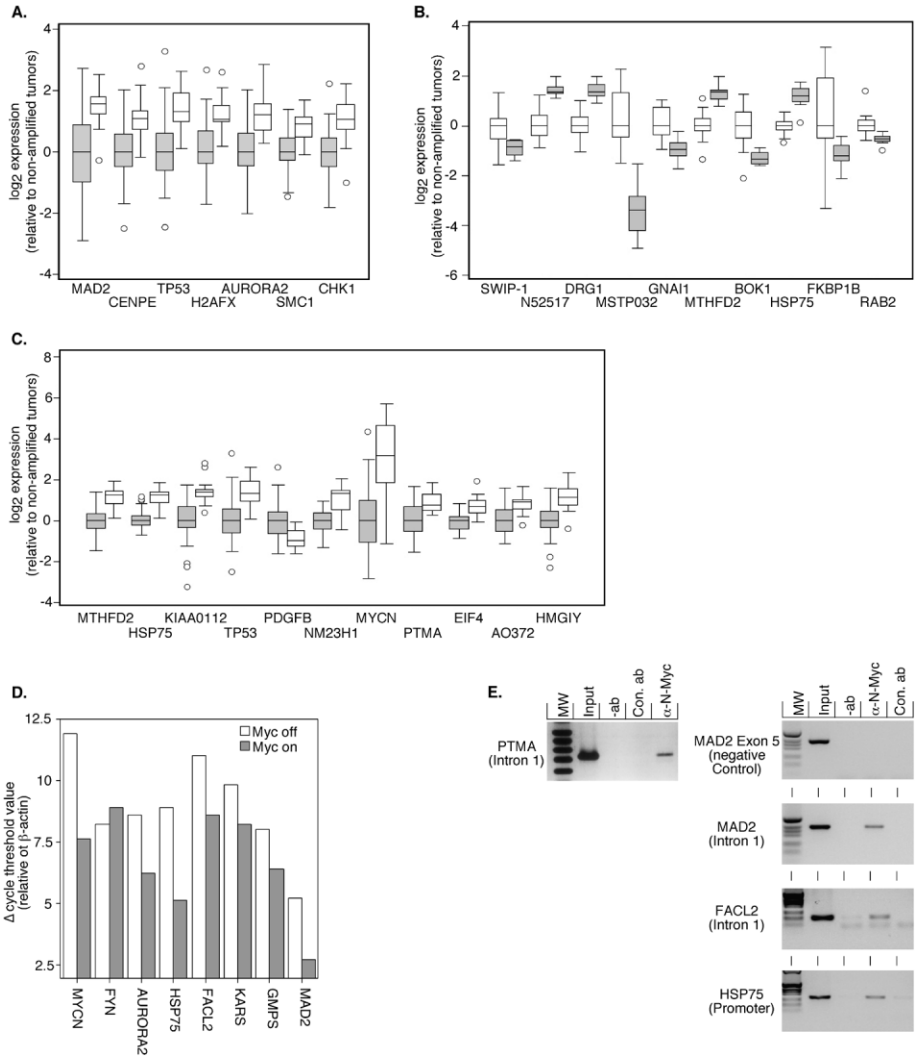

Figure 6. Characterization of genes that are differentially expressed in *MYCN* amplified tumors

A: Boxplots documenting enhanced expression of multiple genes involved in G2 progression and checkpoint functions in *MYCN* amplified tumors (white boxes) versus nonamplified tumors (gray boxes).

B: Boxplots documenting expression of 10 differentially expressed genes in stage 4 tumors, either with (white boxes) or without (gray boxes) amplified *MYCN*. The 10 genes from Supplemental Figure S2 with the lowest p values are shown.

C: Multiple known target genes of Myc are differentially regulated in *MYCN* amplified versus nonamplified tumors. White boxes indicate expression in amplified tumors, gray boxes in nonamplified tumors. All known target genes up to an adjusted p value of $p = 0.05$ are listed. All genes shown are upregulated by Myc in culture with the exception of *PDGFB*, which is repressed by Myc.

D: Multiple genes that are differentially expressed in *MYCN* amplified tumors are regulated by N-Myc in culture. Shown are the results of quantitative PCR experiments documenting expression of the indicated genes in a neuroblastoma cell line carrying a tetracycline-regulatable allele of *MYCN* (Lutz et al., 1996). The plot shows the cycle-threshold value for each gene relative to β-actin.

E: Chromatin immunoprecipitation assays documenting direct binding of N-Myc to E boxes localized in the indicated genes. The left panel shows binding of N-Myc to the E box in the first intron of the *PTMA* gene as positive control (Gaubatz et al., 1994). The right panel shows absence of binding to exon sequences of the *MAD2* genes as negative control. "Con.ab" designates a control antibody, "−ab" designates a control without primary antibody. The position of the E box in each gene is indicated in brackets.

tumors that carry amplified *MYCN* have an extremely poor prognosis, less was known about the factors that control neuroblastoma development in tumors that lack amplified *MYCN*.

We now identify signal transduction through the nonreceptor tyrosine kinase Fyn as one pathway that controls neuroblastoma development in both *MYCN* amplified and nonamplified tumors. This conclusion is based on four lines of evidence. First, array analysis identifies multiple genes that encode proteins, which are functionally linked to *FYN*, as a group of genes coordinately downregulated in advanced stage tumors. Second, Western blotting and kinase assays show that Fyn expression and kinase activity is strongly correlated with tumor stage. Third, expression levels of Fyn predicts prognosis in neuroblastoma. Fourth, active Fyn kinase induces cell cycle arrest and differentiation in cultured neuroblastoma cells.

Several observations suggest that *FYN* regulates neuroblastoma development independently of *MYCN* amplification. For example, expression of Fyn predicts prognosis in tumors that do not carry amplified *MYCN* as well as in the total group of tumors; multivariate analysis indeed shows that expression of Fyn and *MYCN* status are independently prognostic for survival. Consistent with these observations, expression of *FYN* is not significantly different between MYCN amplified and nonamplified tumors. In addition, induction of *MYCN* does not regulate expression of *FYN* in culture. In culture, active Fyn kinase induces cell cycle arrest and morphological differentiation in both neuroblastoma cell lines that do or do not have amplified *MYCN*.

Conversely, microarray analysis defines a distinct group of genes that are differentially regulated in *MYCN* amplified tumors. This set of genes shows almost no overlap with the stage-specific group of genes that point to the role of *FYN* in neuroblastoma. Further analysis suggests that a significant proportion of the genes that are deregulated in *MYCN* amplified tumors are either direct or indirect downstream targets of N-Myc; most likely, therefore, they are regulated in response to *MYCN* amplification. Taken together, our data strongly suggest that signal transduction through Fyn and amplification of *MYCN* define distinct molecular pathways that independently control neuroblastoma development.

FYN is neither mutated nor does it show LOH in neuroblastoma. Therefore, the genetic factors that lead to downregulation of *FYN* expression in advanced stage neuroblastoma remain unclear.

Fyn kinase has been causally implicated in the differentiation

of both oligondendrocytes and keratinocytes (Cabodi et al., 2000; Calautti et al., 1995; Wolf et al., 2001). Downregulation of *FYN* in advanced tumor stages may therefore contribute to the loss of differentiated features and enhanced cell proliferation in advanced tumor stages. In tissue culture and in transgenic mice, signaling through Fyn has also been implicated in neurite extension and cell adhesion (Brouns et al., 2000, 2001). Advanced tumor stages are also characterized by their ability to invade lymph nodes and form metastases. It is also possible, therefore, that downregulation of *FYN* and altered cell adhesion contribute to these invasive properties of neuroblastoma tumors.

Several possibilities exist as to how active *FYN* may exert its function. In neuronal cells, nonreceptor tyrosine kinases phosphorylate Rho-GAP, leading to inactivation of Rho and induction of differentiation (Brouns et al., 2001). In mouse melanocytes, active Fyn kinase induces a lasting activation of the MAPkinase pathway through inhibition of MAPkinase phosphatase 1 (Wellbrock et al., 2002); persistent MAPkinase activation has similarly been shown to induce neuronal differentiation (Qui and Green, 1992). We suggest that downstream signaling molecules that are inhibited by Fyn may be targets for therapeutic intervention in neuroblastoma. For example, Rho exerts its biological functions in part through activation of Rho-kinase (e.g., Sahai and Marshall, 2002). If inhibition of Rho and of Rho-kinase is critical for the effects of *FYN* in neuroblastoma, inhibition of Rho-kinase might mimic the cell cycle arrest and differentiation-inducing effects of Fyn. Similarly, Fyn kinase activity is negatively regulated through phosphorylation of Fyn by Csk in vivo, and inhibition of Csk might therefore lead to activation of endogenous Fyn kinase even when expression levels are low (Imamoto and Soriano, 1993). In this respect, we suggest that interference with signaling through Fyn may provide a therapeutic avenue for advanced stage neuroblastoma.

Experimental procedures

Microarray experiments

The chip we used contains the gf200 set of Research Genetics cDNAs (http://www.resgen.com) and an additional 90 cDNAs that had previously been described as potentially prognostic for neuroblastoma development (for details, see http://www.imt.uni-marburg.de). Each cDNA was spotted twice per chip. Chips were generated as described in Hegde et al. (2000) using a GMS 417 arrayer. All genes that were selected for further analysis were resequenced to confirm their identity.

Initial histochemistry of a series of 100 randomly picked tumors revealed that approximately 95% of the tumors had less than 5% nontumor cells in the biopsies we used (Bergmann et al., 2001 and data not shown). Therefore, no further attempt was made to dissect tumor tissue before preparation of RNA. Total RNA from neuroblastoma tissue and SHEP was isolated using a Qiagen RNA isolation kit according to manufacturers' instructions. 40 μg total RNA was used to synthesize Cy3- and Cy5-fluorescently labeled cDNA according to published protocols (http://brownlab.stanford.edu). Chips were scanned using a GMS 418 fluorescent scanner and the images analyzed using IMAGENE 3.0 software. Expression data were validated using either Northern blot analysis (data not shown) or real-time RT-PCR assays (see Supplemental Figure S1 at http://www.cancercell.org/cgi/content/full/2/5/377/DC1).

Standardization and quality control

ImaGene 3.0. software parameters like "signal range" or "spot detection threshold" (see ImaGene user's manual for details) were optimized for maximum reproducibility prior to the image analysis of our experiment (data not shown). For each spot, median signal and background intensities for both channels were obtained. To account for spot differences, the background corrected ratio of the two channels was calculated and $\log_2$-transformed.

To balance the fluorescence intensities for the two dyes, as well as to allow for comparison of expression levels across experiments, the raw data was standardized. First, we used a pin-wise intensity-dependent standardization (Yang et al., 2002) to correct for inherent bias on each chip (the lowess scatter-plot smoother). In a second step, a global standardization was applied to center the log-ratios for each array at zero (to account for global staining and scanner effects). As each gene was spotted twice on the chip, mean log-ratios M were calculated from replicates. If gene replicates differed more than 4-fold or the background intensity was higher than signal intensity, the gene was excluded on that array.

In total, less than 2% of the genes had to be flagged and filtered out. The correlation coefficient between spot replicas on one chip is between 0.8 and 1.0 for 79% of the chips, and between 0.7 and 0.8 for the remaining.

Statistical analysis

The final data matrix consisted of 4608 standardized gene expressions measurements ($\log_2$-ratios) from 94 individual tumors (with missing values). To compare the expression profile between two independent groups, the two-sample t statistic was used for every gene. To account for multiple testing, we computed adjusted p values for each gene using a step-down permutation algorithm (Westfall and Young, 1993; algorithm 4.1). This strategy has been previously applied to microarrays (Callow et al., 2000). The permutation algorithm provides strong control of the familywise error rate (FWER) and takes into account correlation of the variables (genes). The procedure does not rely upon a normality assumption. Evaluating all genes with an adjusted p value of less than 5%, for example, means that the probability of having one or more false positive genes within the whole list is less than 5%. The log-rank test was used for statistical comparison of survival curves, and Cox's model for multivariate analysis.

Cluster analysis

Prior to the cluster analysis, the expression profile of each gene was standardized to mean 0 and variance 1. Average linkage hierarchical clustering was then performed for genes as well as for chips using the Euclidean distance metric as implemented in the program J-Express (Dysvik and Jonassen, 2001).

Representation of expression data

Expression data of individual genes are shown as box plots. For a detailed description of these plots, see http://www.ruf.rice.edu/~lane/hyperstat/A37797.html. Briefly, the line in the middle represents the median of the expression. The whiskers show the upper and lower range of data, up to 1.5× the box length from the median. The box shows the range of data between the 25th and 75th percentiles. An outlier (more than 1.5× the box length from the median) is shown as a circle.

Real-time RT-PCT analysis

10 μg of total RNA were reverse transcribed using Superscript II Reverse transcriptase and an oligodT_{15} primer according to the manufacturer's instructions. Real time PCR was performed on a Biorad I-Cycler using Sybr Green as detection agent; the products were detected using a 490 nm filter. Primer pairs specific for *AURORA2*, *FACL2*, *FYN*, *GMPS*, *KARS*, *MAD2*, and *MYCN* are available upon request.

Western blots and immunoprecipitation

The following antibodies were used in Western blots, immunofluorescence experiments, and immunoprecipitations: α-Fyn (sc-434), α-cdk2 (sc-163), and α-cyclinA (sc-751) (all Santa Cruz); α-BrdU (Amersham); and α-GAP43 (Novus Biochemicals NB300-1434A1). Neuroblastoma tissue was lysed as described elsewhere (Bergmann et al., 2001).

In vitro kinase assays

500 μg cellular proteins were immunoprecipitated with 5 μg α-Fyn antibody bound to protein G beads, washed and equilibrated in kinase assay buffer, incubated 15 min with 10 μCi γ-ATP (Amersham) and 0.125 mg/ml enolase, electrophoresed on a 10% SDS PAGE, and dried. Results were visualized on a Fuji phosphoimager and quantified using Image Gauge software.

Chromatin immunoprecipitation

Chromatin immunoprecipitation was performed as previously described (Bouchard et al., 2001). Nuclear extracts from IMR-32 were immunoprecipitated overnight at 4°C with 3 μg α-N-Myc antibody or control antibody bound to protein A and G beads. For PCR analysis, specific primer pairs for intron 1 of prothymosin α (as positive control) as well as primer pairs amplifying the indicated genomic regions were used. Primer sequences are available upon request.

Tissue culture experiments

SH-SY5Y and IMR-32 neuroblastoma cell lines were grown in RPMI 1640 supplemented with 10% heat-inactivated FCS. CMV-driven expression constructs encoding Fynwt and FynK299M were a kind gift from M. Resh and have been described (Wolf et al., 2001). Plasmids encoding AFAPΔLZ and AFAPΔ180-226 have been described in Baisden et al. (2001). For transient transfections, cells were first grown on coverslips coated with a 1:5 dilution of Matrigel (Becton-Dickinson) for 6 hr. Transfection was performed using 5 μg of DNA and Lipofectin Reagent (Invitrogen). Cells were fixed with paraformaldehyde after 48 hr, washed, and stained with monoclonal α-Fyn antibody (Santa Cruz) or α-AFAP rabbit-polyclonal antibody (Baisden et al., 2001). BrdU labeling and immunofluorescence of transfected cells was performed as described previously (Rudolph et al., 1996).

For FACSscan analysis, SH-SY5Ycells were transfected with a plasmid encoding a chimerical FYN-EGFP protein (kind gift of Marilyn Resh). 48 hr after transfections, cells were fixed in ethanol and stained with propidium iodide. Samples were gated for GFP-positive and -negative cells and then analyzed separately.

Acknowledgments

This study was supported by grants from the Sander Foundation and the Deutsche Krebshilfe. We thank Marilyn Resh for the kind gift of expression plasmids encoding Fynwt and FynK299M, technical advice on Fyn kinase assays, and the gift of a plasmid encoding FYN-EGFP chimeric proteins. We also thank Manfred Schartl for comments on the manuscript, Stefan Gebhard for help with microarrays, Karin Zamzow for statistical analysis, and Angelika Filmer, Axel Badouin, and Sigrid Bischofsberger for expert technical assistance. This study made use of the J-Express program developed and distributed by Molmine AS and collaborators.

Received: May 30, 2002
Revised: September 18, 2002

References

Baisden, J.M., Gatesman, A.S., Cherezova, L., Jiang, B.H., and Flynn, D.C. (2001). The intrinsic ability of AFAP-110 to alter actin filament integrity is linked with its ability to also activate cellular tyrosine kinases. Oncogene *20*, 6607–6616.

Beier, R., Burgin, A., Kiermaier, A., Fero, M., Karsunky, H., Saffrich, R., Moroy, T., Ansorge, W., Roberts, J., and Eilers, M. (2000). Induction of cyclin E-cdk2 kinase activity, E2F-dependent transcription and cell growth by myc are genetically separable events. EMBO J. *19*, 5813–5823.

Bergmann, E., Wanzel, M., Weber, A., Shin, I., Christiansen, H., and Eilers, M. (2001). Expression of P27(KIP1) is prognostic and independent of MYCN amplification in human neuroblastoma. Int. J. Cancer *95*, 176–183.

Berthold, F., Sahin, K., Hero, B., Christiansen, H., Gehring, M., Harms, D., Horz, S., Lampert, F., Schwab, M., and Terpe, J. (1997). The current contribution of molecular factors to risk estimation in neuroblastoma patients. Eur. J. Cancer *33*, 2092–2097.

Bouchard, C., Dittrich, O., Kiermaier, A., Dohmann, K., Menkel, A., Eilers, M., and Luscher, B. (2001). Regulation of cyclin D2 gene expression by the Myc/Max/Mad network: Myc-dependent TRRAP recruitment and histone acetylation at the cyclin D2 promoter. Genes Dev. *15*, 2042–2047.

Brodeur, G.M., Seeger, R.C., Schwab, M., Varmus, H.E., and Bishop, J.M. (1984). Amplification of N-*myc* in untreated human neuroblastomas correlates with advanced disease stage. Science *224*, 1121–1124.

Brouns, M.R., Matheson, S.F., Hu, K.Q., Delalle, I., Caviness, V.S., Silver, J., Bronson, R.T., and Settleman, J. (2000). The adhesion signaling molecule p190 RhoGAP is required for morphogenetic processes in neural development. Development *127*, 4891–4903.

Brouns, M.R., Matheson, S.F., and Settleman, J. (2001). p190 RhoGAP is the principal Src substrate in brain and regulates axon outgrowth, guidance and fasciculation. Nat. Cell Biol. *3*, 361–367.

Cabodi, S., Calautti, E., Talora, C., Kuroki, T., Stein, P.L., and Dotto, G.P. (2000). A PKC-eta/Fyn-dependent pathway leading to keratinocyte growth arrest and differentiation. Mol. Cell *6*, 1121–1129.

Calautti, E., Missero, C., Stein, P.L., Ezzell, R.M., and Dotto, G.P. (1995). fyn tyrosine kinase is involved in keratinocyte differentiation control. Genes Dev. *9*, 2279–2291.

Calautti, E., Cabodi, S., Stein, P.L., Hatzfeld, M., Kedersha, N., and Paolo Dotto, G. (1998). Tyrosine phosphorylation and src family kinases control keratinocyte cell-cell adhesion. J. Cell Biol. *141*, 1449–1465.

Callow, M.J., Dudoit, S., Gong, E.L., Speed, T.P., and Rubin, E.M. (2000). Microarray expression profiling identifies genes with altered expression in HDL-deficient mice. Genome Res. *10*, 2022–2029.

Clementi, F., Cabrini, D., Gotti, C., and Sher, E. (1986). Pharmacological characterization of cholinergic receptors in a human neuroblastoma cell line. J. Neurochem. *47*, 291–297.

Coller, H.A., Grandori, C., Tamayo, P., Colbert, T., Lander, E.S., Eisenman, R.N., and Golub, T.R. (2000). Expression analysis with oligonucleotide microarrays reveals that MYC regulates genes involved in growth, cell cycle, signaling, and adhesion. Proc. Natl. Acad. Sci. USA *97*, 3260–3265.

Dysvik, B., and Jonassen, I. (2001). J-Express: exploring gene expression data using Java. Bioinformatics *17*, 369–370.

Eggert, A., Grotzer, M.A., Ikegaki, N., Liu, X.G., Evans, A.E., and Brodeur, G.M. (2002). Expression of the neurotrophin receptor TrkA down-regulates expression and function of angiogenic stimulators in SH-SY5Y neuroblastoma cells. Cancer Res. *62*, 1802–1808.

Eilers, M., Schirm, S., and Bishop, J.M. (1991). The MYC protein activates transcription of the alpha-prothymosin gene. EMBO J. *10*, 133–141.

Eisenman, R.N. (2001). Deconstructing myc. Genes Dev. *15*, 2023–2030.

Elend, M., and Eilers, M. (1999). Cell growth: downstream of Myc—to grow or to cycle? Curr. Biol. *9*, R936–R938.

Gaubatz, S., Meichle, A., and Eilers, M. (1994). An E-box element localized in the first intron mediates regulation of the prothymosin α gene by c-myc. Mol. Cell. Biol. *14*, 3853–3862.

Gregorio, C.C., Weber, A., Bondad, M., Pennise, C.R., and Fowler, V.M. (1995). Requirement of pointed-end capping by tropomodulin to maintain actin filament length in embryonic chick cardiac myocytes. Nature *377*, 83–86.

Guo, Q.M., Malek, R.L., Kim, S., Chiao, C., He, M., Ruffy, M., Sanka, K., Lee, N.H., Dang, C.V., and Liu, E.T. (2000). Identification of c-myc responsive genes using rat cDNA microarray. Cancer Res. *60*, 5922–5928.

Hegde, P., Qi, R., Abernathy, K., Gay, C., Dharap, S., Gaspard, R., Hughes, J.E., Snesrud, E., Lee, N., and Quackenbush, J. (2000). A concise guide to cDNA microarray analysis. Biotechniques *29*, 548–550, 552–554, 556

Hiyama, E., Hiyama, K., Yokoyama, T., Matsuura, Y., Piatyszek, M.A., and Shay, J.W. (1995). Correlating telomerase activity levels with human neuroblastoma outcomes. Nat. Med. *1*, 249–255.

Ignelzi, M.A., Jr., Miller, D.R., Soriano, P., and Maness, P.F. (1994). Impaired neurite outgrowth of src-minus cerebellar neurons on the cell adhesion molecule L1. Neuron *12*, 873–884.

Imamoto, A., and Soriano, P. (1993). Disruption of the csk gene, encoding a negative regulator of Src family tyrosine kinases, leads to neural tube defects and embryonic lethality in mice. Cell *73*, 1117–1124.

Jiang, W., and Hunter, T. (1998). Analysis of cell-cycle profiles in transfected cells using a membrane-targeted GFP. Biotechniques *24*, 349–350, 352, 354.

Johnston, L.A., Prober, D.A., Edgar, B.A., Eisenman, R.N., and Gallant, P. (1999). Drosophila myc regulates cellular growth during development. Cell *98*, 779–790.

Lutz, W., Stohr, M., Schurmann, J., Wenzel, A., Lohr, A., and Schwab, M. (1996). Conditional expression of N-myc in human neuroblastoma cells increases expression of alpha-prothymosin and ornithine decarboxylase and accelerates progression into S-phase early after mitogenic stimulation of quiescent cells. Oncogene *13*, 803–812.

Menssen, A., and Hermeking, H. (2002). Characterization of the c-MYC-regulated transcriptome by SAGE: Identification and analysis of c-MYC target genes. Proc. Natl. Acad. Sci. USA *99*, 6274–6279.

Morton, A.J., and Buss, T.N. (1992). Accelerated differentiation in response to retinoic acid after retrovirally mediated gene transfer of GAP-43 into mouse neuroblastoma cells. Eur. J. Neurosci. *4*, 910–916.

Nakagawara, A., Arima, M., Azar, C.G., Scavarda, N.J., and Brodeur, G.M. (1992). Inverse relationship between trk expression and N-myc amplification in human neuroblastomas. Cancer Res. *52*, 1364–1368.

Nakagawara, A., Arima-Nakagawara, M., Scavarda, N.J., Azar, C.G., Cantor, A.B., and Brodeur, G.M. (1993). Association between high levels of expression of the TRK gene and favorable outcome in human neuroblastoma. N. Engl. J. Med. *328*, 847–854.

O'Hagan, R.C., Schreiber-Agus, N., Chen, K., David, G., Engelman, J.A., Schwab, R., Alland, L., Thomson, C., Ronning, D.R., Sacchettini, J.C., et al. (2000). Gene-target recognition among members of the myc superfamily and implications for oncogenesis. Nat. Genet. *24*, 113–119.

Oster, S.K., Marhin, W.W., Asker, C., Facchini, L.M., Dion, P.A., Funa, K., Post, M., Sedivy, J.M., and Penn, L.Z. (2000). Myc is an essential negative regulator of platelet-derived growth factor beta receptor expression. Mol. Cell. Biol. *20*, 6768–6778.

Pahlman, S., Odelstad, L., Larsson, E., Grotte, G., and Nilsson, K. (1981). Phenotypic changes of human neuroblastoma cells in culture induced by 12-O-tetradecanoyl-phorbol-13-acetate. Int. J. Cancer *28*, 583–589.

Qui, M.S., and Green, S.H. (1992). PC12 cell neuronal differentiation is associated with prolonged p21ras activity and consequent prolonged ERK activity. Neuron *9*, 705–717.

Rudolph, B., Zwicker, J., Saffrich, R., Henglein, B., Müller, R., Ansorge, W., and Eilers, M. (1996). Activation of cyclin dependent kinases by Myc mediates transcriptional activation of cyclin A, but not apoptosis. EMBO J. *15*, 3065–3076.

Sahai, E., and Marshall, C.J. (2002). ROCK and Dia have opposing effects on adherens junctions downstream of Rho. Nat. Cell Biol. *4*, 408–415.

Schuhmacher, M., Staege, M.S., Pajic, A., Polack, A., Weidle, U.H., Bornkamm, G.W., Eick, D., and Kohlhuber, F. (1999). Control of cell growth by c-Myc in the absence of cell division. Curr. Biol. *9*, 1255–1258.

Schuhmacher, M., Kohlhuber, F., Holzel, M., Kaiser, C., Burtscher, H., Jarsch, M., Bornkamm, G.W., Laux, G., Polack, A., Weidle, U.H., and Eick, D. (2001). The transcriptional program of a human B cell line in response to Myc. Nucleic Acids Res. *29*, 397–406.

Schwab, M., Alitalo, K., Klempnauer, K.H., Varmus, H.E., Bishop, J.M., Gilbert, F., Brodeur, G., Goldstein, M., and Trent, J. (1983). Amplified DNA with limited homology to myc cellular oncogene is shared by human neuroblastoma cell lines and a neuroblastoma tumour. Nature *305*, 245–248.

Wellbrock, C., Weisser, C., Geissinger, E., Troppmair, J., and Schartl, M. (2002). Activation of p59(Fyn) leads to melanocyte dedifferentiation by influencing MKP-1-regulated mitogen-activated protein kinase signaling. J. Biol. Chem. *277*, 6443–6454.

Westfall, P.H., and Young, S.S. (1993). Resampling-Based Multiple Testing. Examples and Methods for p-Value Adjustment (New York: Wiley)

Wolf, R.M., Wilkes, J.J., Chao, M.V., and Resh, M.D. (2001). Tyrosine phosphorylation of p190 RhoGAP by Fyn regulates oligodendrocyte differentiation. J. Neurobiol. *49*, 62–78.

Yang, Y.H., Dudoit, S., Luu, P., Lin, D.M., Peng, V., Ngai, J., and Speed, T.P. (2002). Normalization for cDNA microarray data: a robust composite method addressing single and multiple slide systematic variation. Nucleic Acids Res. *30*, e15.

Yarmola, E.G., Edison, A.S., Lenox, R.H., and Bubb, M.R. (2001). Actin filament cross-linking by MARCKS: characterization of two actin-binding sites within the phosphorylation site domain. J. Biol. Chem. *276*, 22351–22358.